nature materials

ARTICLES

PUBLISHED ONLINE: 27 NOVEMBER 2011 | DOI: 10.1038/NMAT3176

H-atom relay reactions in real space

T. Kumagai[1†], A. Shiotari[1], H. Okuyama[1]*, S. Hatta[1,2], T. Aruga[1,2], I. Hamada[3], T. Frederiksen[4,5] and H. Ueba[5]

Hydrogen bonds are the path through which protons and hydrogen atoms can be transferred between molecules. The relay mechanism, in which H-atom transfer occurs in a sequential fashion along hydrogen bonds, plays an essential role in many functional compounds. Here we use the scanning tunnelling microscope to construct and operate a test-bed for real-space observation of H-atom relay reactions at a single-molecule level. We demonstrate that the transfer of H-atoms along hydrogen-bonded chains assembled on a Cu(110) surface is controllable and reversible, and is triggered by excitation of molecular vibrations induced by inelastic tunnelling electrons. The experimental findings are rationalized by *ab initio* calculations for adsorption geometry, active vibrational modes and reaction pathway, to reach a detailed microscopic picture of the elementary processes.

Assembling nanoscale structures with atomic-scale precision and controlling their functions are key challenges towards developing molecule-based devices. To this end, the scanning tunnelling microscope (STM) has made it possible to image, manipulate and characterize single atoms and molecules on surfaces[1,2]. Inelastic tunnelling electrons from the tip of an STM can be used as a source of energy to induce adsorbate motions such as hopping[3], rotation[4,5], switching[6,7] and desorption[8], as well as to initiate chemical reactions such as dissociation[9,10], bond formation[11], dehydrogenation[12,13] and *cis–trans* conversion[14]. STM techniques have also been used to study sequential bond dissociation/formation reactions propagating along self-assembled molecular chains[15]. Here we demonstrate a new class of single-molecule chemistry with the STM involving hydrogen bonds[16]. By engineering a platform of H-bonded chains assembled on a Cu(110) surface we are able to transfer an H-atom from one end of the chain to the other. The reaction, triggered by excitation of molecular vibrations, is reversible and occurs along the H-bonds in a sequential fashion by means of the relay mechanism. This class of reaction can be used to transfer single-bit information from one location to another and might provide a way to realize purely mechanical computations, similar to Babbage's difference engine[17], with molecule-based devices.

H-atom/proton transfer through hydrogen bonds plays an essential role in many functional materials, such as proton conductors[18], organic ferroelectric compounds[19], and confined liquids mimicking protein channels[20]. The relay reaction from one molecular unit to the next is considered to involve coordinated, and often complex, rearrangements within the network, and its study dates back to the idea of 'structural diffusion' introduced by Grotthuss two centuries ago to explain the anomalously high mobility of protons in liquid water[21,22]. As microscopic characterization of relay reactions is extremely challenging in complex environments, insight has been inferred from computer simulations[23–25] and spectroscopic techniques[26–28]. H-atom migration by means of the relay mechanism was also observed at solid surfaces[29], where H-atom/proton dynamics and reactions play crucial roles in, for example, electrode chemistry and heterogeneous catalysis.

H-bonded chains, represented as H_2O–$(OH)_n$ ($n = 2$–4), were assembled on Cu(110) using a combination of STM manipulation and controlled dissociation of individual water molecules. As an example, Fig. 1 shows the assembling procedure of H_2O–$(OH)_2$. First, some water molecules were dissociated into hydroxyl (OH) species and subsequently into atomic oxygen, imaged as a round depression on the hollow site (Fig. 1a, right). The chemical identification of these species is detailed in the Supplementary Information. In the next step we manipulated a water molecule, which is imaged as a round protrusion centred on the top site (Fig. 1a left), along the $[1\bar{1}0]$ direction to react with the oxygen atom, thus yielding the H-bonded hydroxyl dimer, $(OH)_2$ (Fig. 1b, right), as represented by the reaction formula: $H_2O + O \rightarrow (OH)_2$. The produced hydroxyl dimer was identified by inelastic electron tunnelling spectroscopy (STM-IETS; ref. 30) and the possibility of a peroxide molecule was ruled out. Our density functional theory (DFT) calculations also show that a peroxide adsorbed on Cu(110) is unstable and spontaneously dissociated into the hydroxyl dimer. Each hydroxyl group is bound in the short-bridge site on adjacent Cu rows and inclined its OH axis along [001] to form a stable H bond within the dimer[30–32]. Finally, a second water molecule was brought to one end of the $(OH)_2$, yielding an H_2O–$(OH)_2$ chain (Fig. 1d–f). These reactions occur spontaneously when the reactants come sufficiently close to each other. Longer H-bonded chains were also assembled, as described in the Supplementary Information.

The structure of the H_2O–$(OH)_2$ chain was determined by DFT calculations, as shown in Fig. 2a,b. The water molecule and hydroxyl groups are bound at short-bridge sites. Figure 2b illustrates how the H bond formed between the water molecule and its neighbouring hydroxyl group results in an oxygen atom distance that is slightly shorter than between two short-bridge sites. The corresponding simulated STM image (Fig. 2c) is characterized by a 'tadpole'-shaped protrusion, with the head and tail appearing over the water molecule and hydroxyl species, respectively, in good

[1]Department of Chemistry, Graduate School of Science, Kyoto University, Kyoto 606-8502, Japan, [2]JST CREST, Saitama 332-0012, Japan, [3]WPI-Advanced Institute for Materials Research, Tohoku University, Sendai 980-8577, Japan, [4]Donostia International Physics Center (DIPC), 20018 San Sebastián, Spain, [5]Division of Nano and New Functional Materials, Graduate School of Science and Engineering, University of Toyama, Toyama 930-8555, Japan. †Present address: Fritz-Haber-Institut der Max-Planck-Gesellschaft, Faradayweg 4-6, 14195 Berlin, Germany. *e-mail: hokuyama@kuchem.kyoto-u.ac.jp.

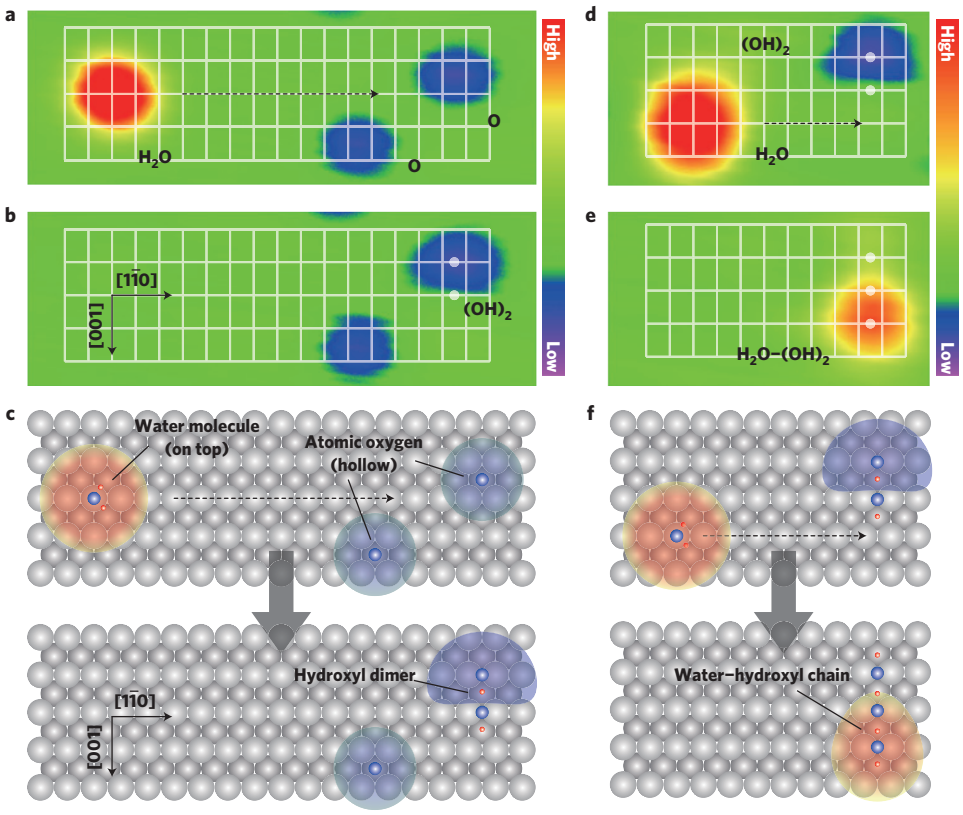

Figure 1 | Sequential STM images of the assembly process of the H_2O-$(OH)_2$ chain from individual water molecules on Cu(110). The images were recorded in constant current mode at a sample bias voltage of $V = 24$ mV and tunnelling current of $I = 0.5$ nA. **a**, A water molecule and two atomic oxygen are imaged as a round protrusion and two depressions, respectively. The white grid lines indicate the lattice of Cu(110). The water molecule was dragged along the [1$\bar{1}$0] direction towards the atomic oxygen (dashed arrow). **b**, The reactants yield an OH dimer, imaged as a semicircular depression. The white dots indicate the short-bridge sites to which the oxygen atoms in $(OH)_2$ are bonded. **c**, Schematic illustration of the reaction process. The light grey circles represent Cu atoms on the substrate, forming 'Cu rows' along the [1$\bar{1}$0] direction. STM images of water, oxygen atoms and $(OH)_2$ are also depicted. **d**, Subsequently, another water molecule was dragged to the end of $(OH)_2$ (dashed arrow). **e**, The reactants yield an H_2O-$(OH)_2$ complex in a chain form. The three dots in **e** depict the nearest short-bridge sites to which oxygen atoms in the complex are bonded. It is noted that the positions of the oxygen atoms deviate slightly from the exact short-bridge sites along the [001] axis, as shown in the structure optimized by DFT calculations (Fig. 2a,b). **f**, Schematic illustration of the reaction process of **d** and **e**. The image sizes are 20×58 Å^2 for **a** and **b**, and 20×36 Å^2 for **d** and **e**.

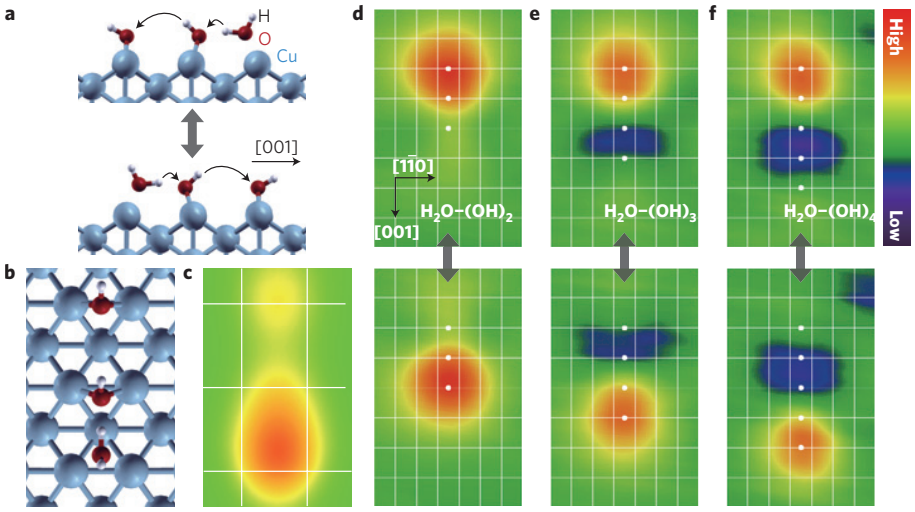

Figure 2 | Assembled water-hydroxyl chains showing H-atom transfer reactions. a, Side view of the H_2O-$(OH)_2$ chain optimized by DFT calculations and its counterpart. **b**, Top view of **a**. **c**, STM simulation for **b**. **d**, Experimental STM images of the H_2O-$(OH)_2$ chain and its counterpart superimposed on the lattice of Cu(110) (white lines). The appearance was inverted by a voltage pulse of the STM over the protrusion. The inversion was also observed for (**e**) H_2O-$(OH)_3$ and (**f**) H_2O-$(OH)_4$ chains. The dots in **d**–**f** indicate the nearest short-bridge sites binding oxygen atoms in the chains (note that oxygen atom positions deviate from the exact short-bridge sites as shown in **b**). The inversion of the appearance corresponds to an H-atom relay reaction in which a sequential H-atom transfer is included, as shown by the curved arrows in **a**. The images were obtained at $V = 24$ mV and $I = 0.5$ nA (18×29 Å^2). The height range shown in the colour scale is from −0.36 to 0.44 Å.

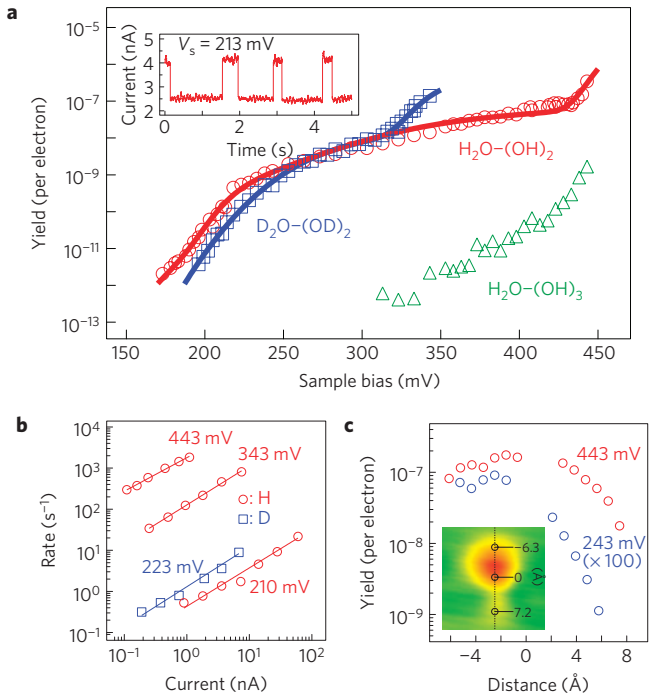

Figure 3 | Yields (rate) of H-atom transfer reactions as a function of voltage, current and position of electron injection. a, Reaction yields as a function of the applied bias voltage. Data were obtained for H_2O-$(OH)_2$ (red circles), D_2O-$(OD)_2$ (blue squares), and H_2O-$(OH)_3$ (green triangles). The inset shows a typical current trace recorded with the tip fixed over the protrusion for H_2O-$(OH)_2$ at $V = 213$ mV. The two-state fluctuation indicates the back-and-forth relay reaction in the chain. The red and blue curves are equation (1) applied to the H_2O-$(OH)_2$ and D_2O-$(OD)_2$ data, respectively, with the following parameters: (mode, $\hbar\Omega_i$/meV, σ^i_{ph}/meV, $e^2K^i_{eff}$) = (H_2O scissors, 213, 11, 6×10^{-9}), (OH* stretch, 310, 38, 18×10^{-8}), (OH stretch, 460, 13, 19×10^{-5}) and (OD* stretch, 262, 23, 6×10^{-8}), (OD stretch, 334, 11, 4×10^{-6}). **b**, The current dependence of the reaction rates for H_2O-$(OH)_2$ (red circles) and D_2O-$(OD)_2$ (blue squares) at various voltages. The slopes were estimated to be 0.82 ± 0.03, 0.95 ± 0.02, 0.97 ± 0.04 and 0.93 ± 0.05 for 443, 343, 223 and 210 mV, respectively. The data are presented in logarithmic scale and the slopes are close to unity, indicating single-electron processes over the whole voltage range. **c**, Position dependence of the yield along the chain for H_2O-$(OH)_2$ at $V = 243$ mV (blue circles) and $V = 443$ mV (red circles). The position is represented by the distance from the centre of the inversion along [001], as shown in the inset with the STM image. Whereas the yield is broadly distributed over the complex at $V = 443$ mV, it is more localized at $V = 243$ mV above the protrusion (water molecule).

agreement with the experimental images. The bright feature in the STM image can thus be assigned to the water molecule in the chain.

A voltage pulse with the STM over the water molecule induced the inversion of the image, which corresponds to H-atom transfer, as shown in Fig. 2d. Detailed analysis of STM images suggested the binding sites of oxygen atoms were not altered during the inversion. This result indicates a mere H-atom relay within the chain, in which intermolecular multiple H-/covalent bond exchange is involved in the process, that moves a water molecule 'apparently' from one end of the chain to the other. This relay reaction occurs in a series of H-bonded chains with varying length (Fig. 2d–f), and is reversible and controllable with the STM. It shares some similarities with the reactions observed in self-assembled CH_3S–SCH_3 aggregates, where S–S bonds were shown to dissociate and form collectively along the chain[15]. However, our H-bonded chains exhibit different dynamics and allow for production of a new water molecule at the end, giving rise to the 'structural' transfer of a water molecule from one end of the chain to the other.

The H-atom transfer can be directly monitored in the current signal of the STM. The inset of Fig. 3a shows the time evolution of tunnelling current measured over the water molecule of H_2O–$(OH)_2$ with the feedback loop open. The high- and low-current states correspond to the initial and final states of the H-atom transfer, respectively, and the jumps in the current are the moments of the transfer event. The transfer rate can be determined from the distribution of time intervals for each event. Any signature of intermediate states, such as the transition state OH–H_2O–OH, was not observed within the timescale of the STM analysis.

To explore the mechanism of the H-atom transfer, the applied bias voltage, tunnelling current (gap resistance) and spatial dependence of the transfer rate was investigated for H_2O–$(OH)_2$, D_2O–$(OD)_2$ and H_2O–$(OH)_3$. In Fig. 3a, the quantum yield (reaction probability per tunnelling electron) of the H-atom transfer is plotted as a function of applied bias voltage. The tip was positioned over the protrusion, that is, the water molecule, during the measurements. Yields were observable at a range from 10^{-12} to 10^{-6} per electron within the experimental timescale. For H_2O–$(OH)_2$ the yield shows an initial increase around 180 mV, a moderate increase beyond ~220 mV, and a sharp enhancement around 430 mV. For D_2O–$(OD)_2$ an isotope effect is observed in which the yield shows an initial increase around 200 mV and a sharp enhancement around 320 mV. The transfer rate shows a linear dependence on the current at several voltages (Fig. 3b), indicating that the transfer is induced by means of single-electron processes over the whole bias range. We confirmed that the same results were obtained with the bias polarity inverted, ruling out that the electric field induces the reaction. These results unambiguously suggest that the H-atom transfer is triggered by the vibrational excitation of the adsorbate molecules.

Figure 3c shows the spatial dependence of the transfer yield at $V = 243$ and 443 mV, where the yield is plotted as a function of the distance along the H-transfer axis ([001] direction), as indicated in the inset. At both voltages the yield is the largest when the tip is positioned over the water molecule, but at $V = 443$ mV it is more broadly distributed over the chain. This indicates that different vibrational modes are involved at these different voltages. The reaction yield was also investigated for H_2O–$(OH)_3$ (Fig. 3a, green triangles) and found to be several orders of magnitude smaller than that of H_2O–$(OH)_2$.

Here we briefly describe a theory to quantify the relation between the transfer yield and vibrational excitation (see also Supplementary Information). The yield $Y(V)$ per electron is defined by $Y(V) = R(V)/I(V)$, where $R(V)$ is the transfer rate and $I(V)$ the tunnel current through the adsorbate at an applied voltage V. The transfer rate induced by single-electron processes can be expressed as $R(V) = K\Gamma_{iet}(V)$, where K is a prefactor determined by the elementary process and Γ_{iet} is the vibrational generation rate[33]. At low temperatures the yield of adsorbate reactions can consequently be written as a sum over contributions from each active vibrational mode[34]

$$Y(V) = \frac{1}{V}\sum_i K^i_{eff}\int_0^{|eV|} d\omega \rho^i_{ph}(\omega)(|eV| - \hbar\omega) \qquad (1)$$

where all voltage-independent parameters are included in effective prefactors K^i_{eff} for each mode i. Also, $\rho^i_{ph}(\omega)$ is the vibrational density of states, which we assume to be normally distributed around the vibrational energy $\hbar\Omega_i$ with a standard deviation σ^i_{ph}. This allows us to take into account vibration broadening effects with the parameter σ^i_{ph}, including finite temperatures, vibrational relaxation, and anharmonic effects of H bonds. As shown by the solid curves in Fig. 3a, equation (1) reproduces the experimental data using the parameters given in the caption. These parameters suggest that three

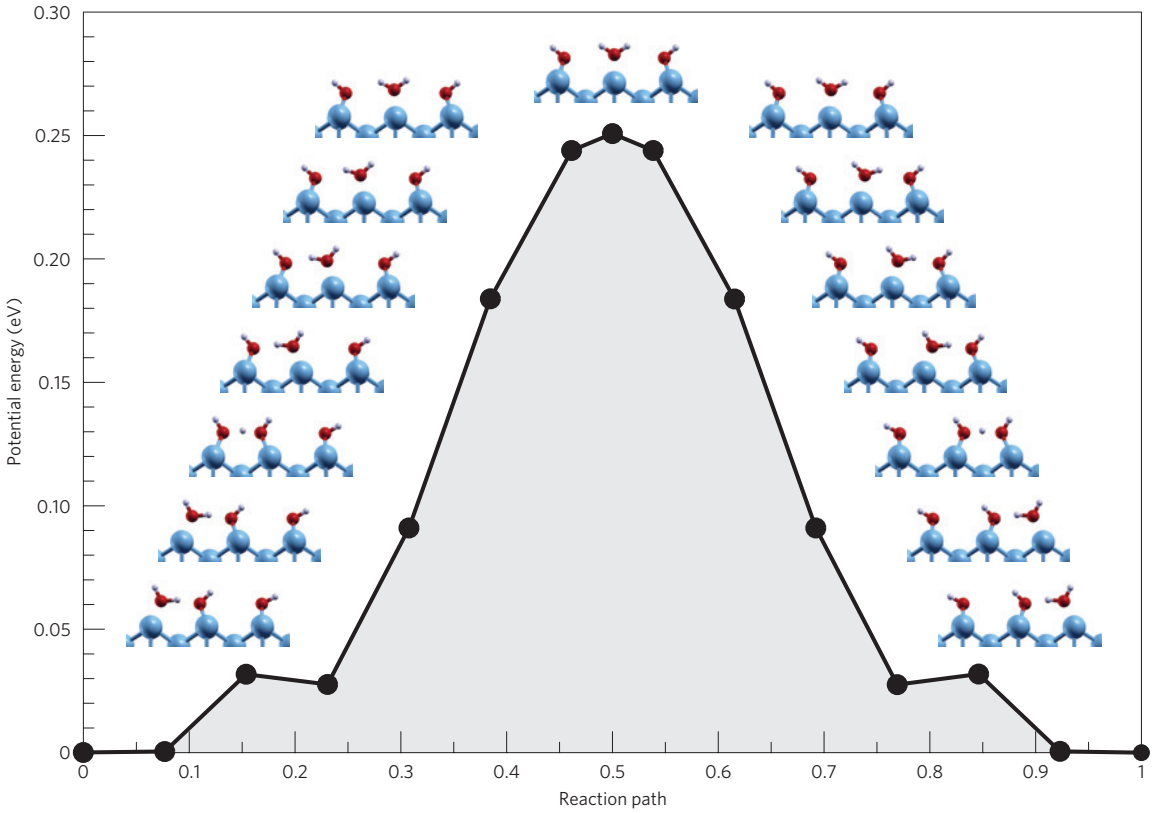

Figure 4 | Calculated potential energy surface for the H-atom relay reaction in an H_2O–$(OH)_2$ chain along the [001] direction. The set of images from initial to final states, shown as insets, were determined by the nudged elastic band method (see Supplementary Information). The H-transfer to the centre OH is easy ($\lesssim$0.04 eV). The transition state (0.25 eV) corresponds to OH–H_2O–OH with a broken H-bond.

characteristic vibrational modes (free OH/OD stretch, OH*/OD* stretch, and H_2O scissors, where H*/D* denotes the shared H/D atom in the H bond) are involved in the relay reaction in the range of voltages where the transfer yield could be observed. The observed onset around 430 [320] mV for H_2O–$(OH)_2$ [D_2O–$(OD)_2$] can be associated with the free OH [OD] stretch mode. At lower voltages we assign modes centred at 310 meV for H_2O–$(OH)_2$ and at 262 meV for D_2O–$(OD)_2$ to shared OH*/OD* stretch modes. In the case of H_2O–$(OH)_2$ also a third mode around 213 meV is taken into account and associated with the H_2O scissors mode. In contrast, for D_2O–$(OD)_2$ the scissors mode is well below the voltage range where the yield is observable. It is noted that the OH*/OD* stretch modes are significantly redshifted from free OH/OD stretch and also characterized by very large broadening (38 meV for OH* and 23 meV for OD*). The significant mode softening with respect to the free stretch modes and spectacular enhancement of the width are familiar from infrared spectroscopy and known to originate in the strong anharmonic character of a single H bond[16]. Both anharmonicity of the mode potential as well as strong coupling to low-energy intermonomer modes affect the detailed features. Furthermore, as anharmonicity is expected to be more pronounced for H than D, the model parameters for OH*/OD* are also consistent with the largest shift and width in the case of OH*.

The vibrational mode analysis also explains why the spatial distribution of the transfer yield (Fig. 3c) is more localized over the water molecule at $V = 243$ mV than at $V = 443$ mV. In the former case, only the H_2O scissors, which is spatially localized within the chain, can be excited. In the latter case, however, also the OH*/OH stretch modes of both the water molecule and hydroxyl groups in the chain can be excited to trigger the transfer, thus resulting in a broader distribution. We note that the dynamics of our H-bond chain reactions, which we have clarified as occurring by direct vibrational excitation, is fundamentally different from reactions induced by purely electronic excitations. For instance, the S–S chain reaction reported in ref. 15 is consistent with an electronic mechanism where the dissociation is initiated by temporal attachment of an electron to an antibonding orbital localized on the S–S bond.

We also investigated the reaction pathway from total energy calculations for the H-atom transfer reaction (Fig. 4). The initial step is transportation of the shared H-atom to the centre hydroxyl, which is almost barrier-less ($\lesssim$0.04 eV). This is in line with the recent DFT calculations that predicted that H-atom sharing in the water and hydroxyl overlayers is easy owing to the quantum nature of the nuclear motion[35]. The subsequent H-bond cleavage between OH and the centre water molecule constitutes the highest barrier of 0.25 eV, in which the displacement of the centre water molecule along the [001] direction is mainly involved. The OH, OH* stretch and H_2O scissors modes are therefore postulated to couple to the reaction coordinate for the H-bond cleavage. It is noted that the H-atom transfer was observed below bias voltages of 250 mV in the bias voltage dependence (Fig. 3a), where the tunnelling electron should not have enough energy to induce the H-atom transfer by means of a merely over-barrier process. We propose that the H-bond cleavage, which mainly involves rotational motion of the centre water molecule, might proceed here by means of vibrationally assisted tunnelling[36] of an entire H_2O or D_2O molecule through the transition state. We found that the imaginary mode of the transition state corresponds to the rotation-translation of the centre water molecule (Supplementary Figs S7 and S9), suggesting that the tunnelling object must be the entire molecule. The transfer reaction is therefore completed either by means of tunnelling (at low bias) or over-barrier processes (at high bias). For the longer chains H_2O–$(OH)_{3,4}$, the H-atom transfer reaction occurs in sequence, and thus the energy dissipation is more

significant, giving rise to lower reaction yields than for H_2O–$(OH)_2$. Such energy dissipation plays a crucial role in determining the product, yield and pathway in chemical reactions on surfaces. Our results in a well-characterized environment thus shed new light on the exploration of the fundamental mechanism of H-atom transfer.

We have demonstrated a vibrationally induced H-atom relay reaction within H-bonded chains assembled on Cu(110) at 6 K using STM techniques. In this reaction H-atom transfer results in the 'structural' transfer of a water molecule from one end of the chain to the other without changing the platform of the chain. These artificial H-bonded chains enabled us to study intermolecular reaction processes, including multiple H-/covalent bond exchange at a single-molecule limit. Engineering even longer and more sophisticated H-bond systems supported on solid surfaces could provide an opportunity not only to achieve mechanical logic circuits using H-atoms but also to systematically study the fundamental steps of H-atom dynamics in heterogeneous systems. Such systems are conceivable by combining the self-assembling nature of water/hydroxyl complexes[37–39] with STM manipulation techniques[40]. Our discovery that H-atom transfer along H-bonds is possible directly on metal surfaces suggests that relay reactions may occur more generally at metal–molecule interfaces and, therefore, in liquids all the way down to the confining surfaces. This is of importance in diverse fields, such as nanofluidics and the design of hybrid materials for proton conduction.

Methods

Experimental. The experiments were performed in an ultra-high vacuum chamber equipped with an STM operating at 6 K. The Cu(110) surface was cleaned by repeated cycles of argon-ion sputtering and annealing. The surface was exposed to H_2O or D_2O gases at 12 K using a tube doser positioned ~1 cm away from the sample surface. The molecules were imaged mainly as isolated monomers after the exposure. By applying $V = 2$ V and $I = 20$ nA to a water molecule, we induced its dissociation into a hydroxyl[30]. The hydroxyl group was further dissociated into atomic oxygen by applying $V = 0.9$ V and $I = 10$ nA.

We conducted the lateral manipulation of a water molecule by decreasing the tunnel resistance to ~1 MΩ, bringing the tip close to a water molecule, and then moving the tip laterally at ~0.1 nm s^{-1} in the $[1\bar{1}0]$ or $[\bar{1}10]$ direction (along the Cu row of the substrate) with the feedback maintained[40]. Although manipulation of a water molecule was conducted in a controlled way, that of an isolated hydroxyl group is not feasible. Nevertheless, its complex with water (H_2O–OH) can be moved along the $[1\bar{1}0]$ direction by applying ~450 mV (Supplementary Fig. S2). In this way, we were able to construct hydrogen-bonded complexes with specific compositions and structures.

Computational. The atomic structure was determined using Kohn–Sham DFT with a plane-wave basis and the Perdew–Burke–Ernzerhof generalized gradient approximation (PBE-GGA) exchange correlation functional[41], as detailed in the Supplementary Information. STM images were simulated with the STATE (Simulation Tool for Atom Technology) code[42–44] within the Tersoff–Hamann theory[45]. Phonon modes and harmonic frequencies were calculated by finite differences. The reaction barrier was estimated using the nudged elastic band (NEB) method[46] as implemented in VASP (Vienna ab-initio simulation package; refs 47–49).

Received 10 June 2011; accepted 20 October 2011; published online 27 November 2011

References

1. Eigler, D. M. & Schweizer, E. K. Positioning single atoms with a scanning tunnelling microscope. *Nature* **344,** 524–526 (1990).
2. Heinrich, A. J., Lutz, C. P., Gupta, J. A. & Eigler, D. M. Molecule cascades. *Science* **298,** 1381–1387 (2002).
3. Komeda, T., Kim, Y., Kawai, M., Persson, B. N. J. & Ueba, H. Lateral hopping of molecules induced by excitation of internal vibration mode. *Science* **295,** 2055–2058 (2002).
4. Stipe, B. C., Razaei, M. A. & Ho, W. Inducing and viewing the rotational motion of a single molecule. *Science* **279,** 1907–1909 (1998).
5. Stipe, B. C., Razaei, M. A. & Ho, W. Coupling of vibrational excitation to the rotational motion of a single adsorbed molecule. *Phys. Rev. Lett.* **81,** 1263–1266 (1998).
6. Liljeroth, P., Repp, J. & Meyer, G. Current-induced hydrogen tautomerization and conductance switching of naphthalocyanine molecules. *Science* **317,** 1203–1206 (2007).
7. Tomatsu, K. *et al.* An atomic seesaw switch formed by tilted asymmetric Sn–Ge dimers on a Ge (001) surface. *Science* **315,** 1696–1698 (2007).
8. Pascual, J. I., Lorente, N., Song, Z., Conrad, H. & Rust, H-P. Selectivity in vibrationally mediated single-molecule chemistry. *Nature* **423,** 525–528 (2003).
9. Stipe, B. C. *et al.* Single-molecule dissociation by tunneling electrons. *Phys. Rev. Lett.* **78,** 4410–4413 (1997).
10. Shin, H-J. *et al.* State-selective dissociation of a single water molecule on an ultrathin MgO film. *Nature Mater.* **9,** 442–447 (2010).
11. Ho, W. Single-molecule chemistry. *J. Chem. Phys.* **117,** 11033–11061 (2002).
12. Katano, S., Kim, Y., Hori, M., Trenary, M. & Kawai, M. Reversible control of hydrogenation of a single molecule. *Science* **316,** 1883–1886 (2007).
13. Kim, Y., Komeda, T. & Kawai, M. Single-molecule reaction and characterization by vibrational excitation. *Phys. Rev. Lett.* **86,** 126104 (2002).
14. Henzl, J., Mehlhorn, M., Gawronski, H., Rieder, K-H. & Morgenstern, K. Reversible cis–trans isomerization of a single azobenzene molecule. *Angew. Chem. Int. Edn Engl.* **45,** 603–606 (2006).
15. Maksymovych, P., Sorescu, D. C., Jordan, K. D. & Yates, J. T. Jr Collective reactivity of molecular chains self-assembled on a surface. *Science* **322,** 1664–1667 (2008).
16. Maréchal, Y. *The Hydrogen Bond and the Water Molecule* (Elsevier, 2007).
17. Swada, D. D. *The Difference Engine: Charles Babbage and the Quest to Build the First Computer* (Penguin, 2002) reprint.
18. Bureekaew, S. *et al.* One-dimensional imidazole aggregate in aluminium porous coordination polymers with high proton conductivity. *Nature Mater.* **8,** 831–836 (2009).
19. Horiuchi, S. & Tokura, Y. Organic ferroelectrics. *Nature Mater.* **7,** 357–366 (2008).
20. Duan, C. & Majumdar, A. Anomalous ion transport in 2-nm hydrophilic nanochannels. *Nature Nanotech.* **5,** 848–852 (2010).
21. Bernal, J. D. & Fowler, R. H. A theory of water and ionic solution, with particular reference to hydrogen and hydroxyl ions. *J. Chem. Phys.* **1,** 515–548 (1933).
22. Agmon, N. The Grotthuss mechanism. *Chem. Phys. Lett.* **244,** 456–462 (1995).
23. Ando, K. & Hynes, J. T. Molecular mechanism of HCl acid ionization in water: *Ab initio* potential energy surfaces and Monte Carlo simulations. *J. Phys. Chem. B* **101,** 10464–10478 (1997).
24. Marx, D., Tuckerman, M. E., Hutter, J. & Parrinello, M. The nature and transport mechanism of hydrated hydroxide ions in aqueous solution. *Nature* **397,** 601–604 (1999).
25. Swanson, J. M. J. *et al.* Proton solvation and transport in aqueous and biomolecular systems: Insights from computer simulations. *J. Phys. Chem. B* **111,** 4300–4314 (2007).
26. Tanner, C., Manca, C. & Leutwyler, S. Probing the threshold to H atom transfer along a hydrogen-bonded ammonia wire. *Science* **302,** 1736–1739 (2003).
27. Mohammed, O. F., Pines, D., Dreyer, J., Pines, E. & Nibbering, E. T. J. Sequential proton transfer through water bridges in acid-base reactions. *Science* **310,** 83–86 (2005).
28. Sakota, K., Inoue, N., Komoto, Y. & Sekiya, H. Cooperative triple-proton/hydrogen atom relay in 7-azaindole$(CH_3OH)_2$ in the gas phase: Remarkable change in the reaction mechanism from vibrational-mode specific to statistical fashion with increasing internal energy. *J. Phys. Chem. A* **111,** 4596–4603 (2007).
29. Nagasaka, M., Kondoh, H., Amemiya, K., Ohta, T. & Iwasawa, Y. Proton transfer in a two-dimensional hydrogen-bonding network: Water and hydroxyl on a Pt(111) surface. *Phys. Rev. Lett.* **100,** 106101 (2008).
30. Kumagai, T. *et al.* Tunneling dynamics of a hydroxyl group adsorbed on Cu(110). *Phys. Rev. B* **79,** 035423 (2009).
31. Tang, Q-L. & Chen, Z-X. Influence of aggregation, defects, and contaminant oxygen on water dissociation at Cu(110) surface: A theoretical study. *J. Chem. Phys.* **127,** 104707 (2007).
32. Ren, J. & Meng, S. First-principles study of water on copper and noble metal (110) surfaces. *Phys. Rev. B* **77,** 054110 (2008).
33. Tikhodeev, S. G. & Ueba, H. Relation between inelastic electron tunneling and vibrational excitation of single adsorbates on metal surfaces. *Phys. Rev. B* **70,** 125414 (2004).
34. Motobayashi, K., Kim, Y., Ueba, H. & Kawai, M. Insight into action spectroscopy for single molecule motion and reactions through inelastic electron tunneling. *Phys. Rev. Lett.* **105,** 076101 (2010).
35. Li, X-Z., Probert, M. I. J., Alavi, A. & Michaelides, A. Quantum nature of the proton in water-hydroxyl overlayers on metal surfaces. *Phys. Rev. Lett.* **104,** 066102 (2010).
36. Tikhodeev, S. G. & Ueba, H. How vibrationally assisted tunneling with STM affects the motions and reactions of single adsorbates. *Phys. Rev. Lett.* **102,** 246101 (2009).
37. Yamada, T., Tamamori, S., Okuyama, H. & Aruga, T. Anisotropic water chain growth on Cu(110) observed with scanning tunneling microscopy. *Phys. Rev. Lett.* **96,** 036105 (2006).
38. Lee, J., Sorescu, D. C., Jordan, K. D. & Yates, J. T. Jr Hydroxyl chain formation on the Cu(110) surface: Watching water dissociation. *J. Phys. Chem. C* **112,** 17672–17677 (2008).

39. Carrasco, J. *et al.* A one-dimensional ice structure built from pentagons. *Nature Mater.* **8,** 427–431 (2009).
40. Kumagai, T., Okuyama, H., Hatta, S., Aruga, T. & Hamada, I. Water clusters on Cu(110): Chain versus cyclic structures. *J. Chem. Phys.* **134,** 024703 (2011).
41. Perdew, J. P., Burke, K. & Ernzerhof, M. Generalized gradient approximation made simple. *Phys. Rev. Lett.* **77,** 3865–3868 (1996).
42. Morikawa, Y., Ishii, H. & Seki, K. Theoretical study of *n*-alkane adsorption on metal surfaces. *Phys. Rev. B* **69,** 041403(R) (2004).
43. Otani, M. & Sugino, O. First-principles calculations of charged surfaces and interfaces: A plane-wave nonrepeated slab approach. *Phys. Rev. B* **73,** 115407 (2006).
44. Hamada, I., Otani, M., Sugino, O. & Morikawa, Y. Green's function method for elimination of the spurious multipole interaction in the surface/interface slab model. *Phys. Rev. B* **80,** 165411 (2009).
45. Tersoff, J. & Hamann, D. R. Theory and application for the scanning tunneling microscope. *Phys. Rev. Lett.* **20,** 1998–2001 (1983).
46. Mills, G., Jónsson, H. & Schenter, G. K. Reversible work transition state theory: Application to dissociative adsorption of hydrogen. *Surf. Sci.* **324,** 305–337 (1995).
47. Kresse, G. & Hafner, J. *Ab initio* molecular dynamics for liquid metals. *Phys. Rev. B* **47,** 558–561 (1993).
48. Kresse, G. & Furthmüller, J. Efficient iterative schemes for *ab initio* total-energy calculations using a plane-wave basis set. *Phys. Rev. B* **54,** 11169–11186 (1996).
49. Kresse, G. & Joubert, D. From ultrasoft pseudopotentials to the projector augmented-wave method. *Phys. Rev. B* **59,** 1758–1775 (1999).

Acknowledgements

We thank the Supercomputer Center, Institute for Solid State Physics, University of Tokyo, and the Information Technology Center, University of Tokyo, for the use of the facilities. H.O. was supported in part by the Grant-in-Aid for Scientific Research on Priority Areas 'Molecular Science for Supra Functional Systems' from the Ministry of Education, Culture, Sports, Science and Technology, Japan. I.H. was supported by the Grant-in-Aid from the Ministry of Education, Culture, Sports, Science and Technology (MEXT), Japan (No. 21740228). H.U. was supported by the Grant-in-Aid for Scientific Research B (No. 18340085) from the Japan Society for the Promotion of Science (JSPS). T.K. acknowledges the support of the JSPS.

Author contributions

T.K. and H.O. designed and planned the experiments. T.K. and A.S. measured and analysed the STM data. I.H. performed the STATE calculations. T.F. performed the VASP calculations. H.O. supervised the project and H.U. provided guidance for the analysis completed by I.H. and T.F. All authors contributed to the discussion of the results. H.O., I.H., T.F. and H.U. wrote the paper.

Additional information

The authors declare no competing financial interests. Supplementary information accompanies this paper on www.nature.com/naturematerials. Reprints and permissions information is available online at http://www.nature.com/reprints. Correspondence and requests for materials should be addressed to H.O.